applied sciences

MDPI

Article

Cooperative Guidance Law for the Mother-Cabin of the Anti-UAV Cluster Mother-Son Missile

Ruining Luo [1], Guangjun He [2,*], Xiangwei Bu [2] and Jianjun Shi [2]

[1] Graduate College, Air Force Engineering University, Xi'an 710051, China; luo_ruining@163.com
[2] Air and Missile Defense College, Air Force Engineering University, Xi'an 710051, China
* Correspondence: 15619013868@163.com

Featured Application: The proposed method can provide a special cooperative guidance law for intercepting a cluster of UAVs using mother-son missiles. Additionally, it provides ideas for methods of counteracting UAV clusters.

Abstract: This article investigates a novel operational pattern for intercepting UAV clusters over the range of middle and far distances using mother-son missiles. To address the guidance issue of the mother-cabin in the operational pattern, a special cooperative guidance law, which takes into account acceleration constraint and satisfies the constraints of impact time, speed, and zero line of sight angle (LOS), is proposed. Based on consistency theory and sliding mode control theory, the proposed cooperative guidance law is specifically designed for the mother-cabin of the mother-son missile. This approach offers several advantages, including a simple structure and smooth controller output, and smooth flight trajectory. Finally, numerical simulations are presented to demonstrate the effectiveness and applicability of the cooperative guidance law.

Keywords: cooperative guidance; mother-son missile; consistency theory; sliding mode control; acceleration constraint

Citation: Luo, R.; He, G.; Bu, X.; Shi, J. Cooperative Guidance Law for the Mother-Cabin of the Anti-UAV Cluster Mother-Son Missile. *Appl. Sci.* **2023**, *13*, 5397. https://doi.org/10.3390/app13095397

Academic Editor: Jérôme Morio

Received: 28 March 2023
Revised: 22 April 2023
Accepted: 23 April 2023
Published: 26 April 2023

1. Introduction

In order to effectively execute the missions, missiles need to cooperate in certain ways due to diverse operational tasks and increasingly complicated operational environments. The current research priority in cooperative guidance is to develop effective cooperative guidance strategies based on advanced information and communication technologies for specific combat scenarios. This ensures that multiple missiles can impact targets in the most optimal state under specified flight times, impact angles, and other constraints.

Jeon et al. [1] first proposed a cooperative guidance method based on time coordination, which adds the time-to-go error feedback term to the traditional guidance loop. This method realizes the flight time control by adding a correction term to the guidance output of the proportional guidance method based on the background of multi-missile coordinated impact warship. Based on the same methodology, they proposed a cooperative guidance law considering impact angle and time constraints, and further restricted the impact angle [2]. In [3,4], the time error and angle error feedback terms were superimposed on the offset proportional guidance method to propose the cooperative guidance law with impact time and angle constraints. For the above strategies, the impact time must be specified in advance. The state of each missile will not be changed dynamically, and the missile does not communicate while it is in the air. Therefore, they do not exhibit genuine coordination. These techniques, sometimes known as independent cooperative guidance or open-loop cooperative guidance [5], suffer from limited intelligence and weak robustness.

The primary focus of current research is on integrated/closed-loop cooperative guidance based on information exchange among missiles. The "leader-follower" cooperative guidance structure [6] or the two-layer cooperative guidance structure [7] is used as a framework for most cooperative approaches. Both homogeneous and heterogeneous missiles can theoretically cooperate based on the two architectures, but in practice, the "leader-follower" structure is more appropriate for heterogeneous missiles and has the advantages of good real-time information, easy expansion of missile groups, and high economic benefits [8–11]. The two-layer structure is suitable for both homogeneous and heterogeneous missiles with its flexible cooperative mode and strong robustness [12–14]. Cooperative design based on sliding mode control theory has become a popular research area, in addition to the cooperative guidance method design based on optimal control theory and the proportional navigation method. In recent years, consistency theory has been introduced into the development of cooperative methods [15–18]. This theory has been combined with the theory of sliding mode control, using a non-singular terminal sliding mode [19–21] or a super-twisting sliding mode control [22,23] which can achieve fast convergence of missile states with reduced output chattering. Reference [24] proposed a prescribed performance-based approach for the cooperative control of missile flight angles. For practical problems such as the fragility of the prescribed performance approach and the high-complexity of neural prescribed performance control, Bu et al. proposed non-fragile and low-complexity prescribed performance approaches [25–29], which provide advanced approaches to the design of prescribed performance-based cooperative control laws. While controlling multiple missiles for tactical cooperation, reference [30,31] furthered the design of collision avoidance between multiple missiles. While most of the solutions to the controller are based on quadratic Lyapunov functions, reference [32,33] considered a non-quadratic Lyapunov function with one degree of freedom denoted as α and showed that they had a much faster response. Among them, most of the cooperative guidance laws have been designed for specific application scenarios, and the guidance effect cannot be guaranteed after changing the application scenario. These laws also take less account of acceleration constraints and the feasibility of flight trajectories. As a result, it is necessary to design a special cooperative guidance law that is tailored to specific operational contexts and can meet specific constraints while taking into account practical constraints such as acceleration limits and flight trajectories.

Numerous academic and research organizations have conducted studies on UAV countermeasures in response to the growing threat posed by them. Based on the current state of research, hard kill methods such as firearms, artillery, directed energy weapons and UAV cluster countermeasures have been proposed to directly destroy targets, as well as soft kill methods such as communication jamming, photoelectric decoys and electromagnetic bomb to paralyse cluster warfare capabilities.Most current plans aim to develop a defense system with a combination of hard and soft killing means with echelon deployment, and use a variety of means to effectively counter UAV clusters [34–36]. These strategies have been developed due to the effectiveness of individual means and the constraints of use conditions. The effective range of these weapons for UAV detection, interference, and killing is typically between 5 km and 25 km, and the suggested defense systems can only achieve medium- to short-range protection. Another efficient strategy is to use conventional air defense systems to intercept the carrier aircraft and completely destroy the cluster. However, there is less research on countermeasures for UAV clusters in the medium- and far-range formation cruise phase after the release of the carrier aircraft.

The main contributions of this study are as follows:

(1) We propose a novel pattern of intercepting UAV cluster: the use of mother-son missiles to in-tercept UAV cluster composed of medium to large UAVs over the range of medium and far distances.
(2) For the proposed operational pattern, we have designed a special guidance law for the mother-cabins of the mother-son missiles with the following characteristics: zero LOS constraint, smooth convergence of each missile velocity, and converge to the same velocity only at the time of impacting the targets. This design allows the controller to

have a small and smooth output. In addition, given the weak cluster mobility of the UAV cluster, the controller designed in this paper is simple and easy to implement.

2. Description and Analysis of Cooperative Guidance of Multiple Mother-Cabins

2.1. The Operational Pattern of Cooperative Interception of UAV Clusters by Mother-Son Missiles

When a UAV cluster carries out a combat mission, it can generally be divided into the following four phases: first, the carrier aircraft releases the UAVs outside the defense area at a long distance. Then, the UAVs assemble, form up, and fly intensively, and then fly in scattered formations to the mission area. Finally, the UAVs carry out combat missions such as detection, interference, and attack according to the established plan. Among these phases, during the phase of formation and intensive flight over the range of medium and far distances, the communication and coordination functions of the cluster are not yet complete, which is the weakest stage of protection capability. At this stage, the formation is dense, and the cluster as a whole has a weak maneuverability due to the performance of the individual UAVs and the constraints of the formation structure.

Based on the above characteristics of the cluster, an operational pattern of intercepting UAV clusters over the range of medium and long distances (the phase of formation and intensive flight) by using mother-son missiles is proposed. The mother-son missile in this pattern consists of a turbojet-powered mother-cabin and non-powered son-interceptors carried in the mother-cabin. The targets of interception are medium to large sized UAVs used for cluster combat. Such targets have a long combat range and high altitude, and their payload capacity is sufficient to enable them to perform various combat roles such as reconnaissance, interference, and attack, which pose a high threat level and intercept utility.

The basic interception strategy is to select high-threat targets within the cluster and divide the selected targets into multiple sub-clusters based on the interception capability of each mother-son missile. Each mother-son missile is then responsible for intercepting one sub-cluster. The basic interception process involves calculating the position of the "release point" of each mother-cabin in real time according to the motion state information of each sub-cluster threat's "center of gravity". The mother-cabin performs a guided flight according to the "release point" and releases the son-interceptor after arriving at the "release point". The son-interceptors intercept the designated UAV targets. The basic operational concept is shown in Figure 1. The threat "center of gravity" is a spatial particle inside the cluster, which is used to represent the location of the cluster. The "release point" is a spatial particle derived from the threat "center of gravity" along the horizontal direction. In order to emphasize the research on the cooperative guidance law of the mother-cabin, this paper will not discuss the method of cluster clustering or the calculation methods of the threat "center of gravity" and "release point".

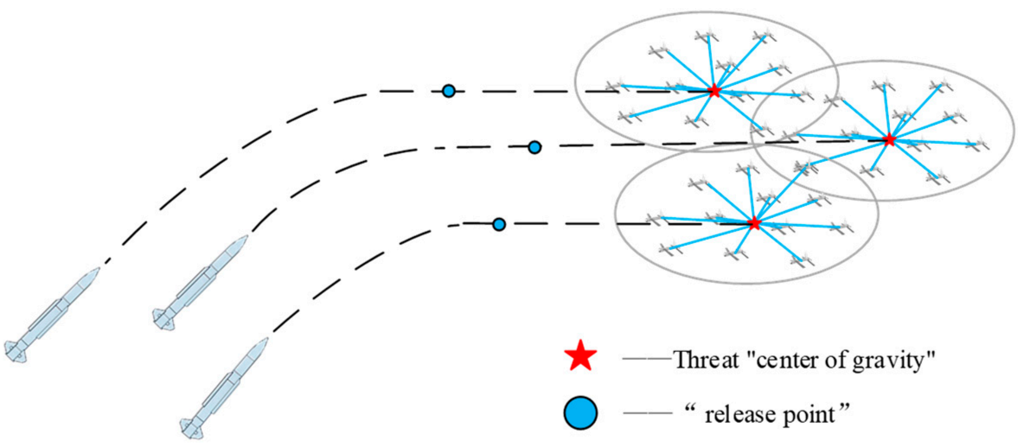

Figure 1. Multiple mother-son missiles intercepting UAV clusters.

2.2. Analysis of the Mother-Cabin Guidance

The guidance phase of the mother-cabin refers to the phase in which the mother-cabin flies to the "release point" according to the constraint requirements. The mother-cabin guidance is a key link in the whole interception process. The result of the mother-cabin guidance is related to whether the mother-cabin seeker can track the targets stably and release the son-interceptors effectively. The mother-cabin guidance should meet two requirements:

First, the impact process between the son-interceptors and the targets will produce complex infrared features and more target-points in the air, which will interfere with the subsequent identification and interception of the UAV targets by the mother-cabin and son-interceptors. Therefore, it is hoped that multiple mother-cabins will reach the "release point" at the same time and release the son-interceptors at the same speed to achieve simultaneous interception of the target.

Second, considering the detection of the target by the mother-cabin, the LOS of the mother-cabin to the "release point" must converge to zero before reaching the "release point". This ensures that the carried composite seeker has been aligned with the cluster before reaching the "release point" so as to achieve the track of the target as quickly as possible.

Based on the above two constraints, this paper designs a multi-missile cooperative guidance law that satisfies the constraints of impact time, speed, and zero LOS. In the design of the guidance law, this paper draws on consistency theory and sliding mode control theory, which are currently more widely used in state-of-the-art methods. Because of the weak maneuverability of UAV cluster, it is relatively easy to achieve the interception. In view of this, we try to obtain a simpler controller structure, smooth controller output, and smooth trajectory while still satisfying the guidance constraints.

Remark 1. *Considering the simplicity of the analysis process, this paper discusses the guidance law of the mother-cabin in the two-dimensional plane. If it is in the three-dimensional plane, the "zero LOS constraint" mentioned above should be described as follows: the mother-cabin should be at the same height as the cluster, and the direction of speed should be the direction of the line connecting the "release point" and the cluster threat "center of gravity". The expression of other constraints remains unchanged. The "release point" changes with the movement of the cluster, which can be regarded as a maneuvering target for the guidance of the mother-cabin. For the sake of readability, the "release point" will be collectively referred to as the target, and the mother-cabin will be collectively referred to as the missile in the following text.*

2.3. Missile-Target Relative Motion Model

In the longitudinal plane, the relative motion model for the cooperative interception of multiple maneuvering targets by multiple missiles is shown in Figure 2.

In Figure 2, both the missile and the target are in the inertial frame, where M_1, M_2, and M_3 represent three missiles, T_1, T_2, and T_3 represent three guidance targets, v_i and α_i represent the velocity and normal acceleration of missile i, θ_i, and q_i represent the trajectory inclination angle and LOS of the missile i, v_{Ti}, and θ_{Ti} represent the velocity and trajectory inclination angle of the target i, and r_i is the relative distance between the missile and the target.

Remark 2. *The trajectory inclination angle θ and the LOS q rotate counterclockwise along the reference direction to be positive, and the value range is $-180^\circ \sim 180^\circ$.*

Although the angular relationship between different missiles and targets is different, the relative motion relationship between them can be expressed by the following general equation:

$$\begin{cases} r_i\dot{q}_i = -v_{Ti}\sin(q_i - \theta_{Ti}) + v_i\sin(q_i - \theta_i) \\ \dot{r}_i = v_{Ti}\cos(q_i - \theta_{Ti}) - v_i\cos(q_i - \theta_i) \end{cases} \tag{1}$$

By applying the derivative operation to $\dot{r}$ and $\dot{q}$ in Equation (1), we obtain:

$$\begin{cases} \ddot{r}_i = r_i\dot{q}_i^2 - u_{ri} + w_{ri} \\ \ddot{q}_i = -2\frac{\dot{r}_i\dot{q}_i}{r_i} - \frac{u_{qi}}{r_i} + \frac{w_{qi}}{r_i} \end{cases} \tag{2}$$

where $w_{ri} = \dot{v}_{Ti}\cos(q_i - \theta_{Ti}) + v_{Ti}\dot{\theta}_{Ti}\sin(q_i - \theta_{Ti})$ and $w_{qi} = -\dot{v}_{Ti}\sin(q_i - \theta_{Ti}) + v_{Ti}\dot{\theta}_{Ti}$ $\cos(q_i - \theta_{Ti})$ are the acceleration of the target in the direction of LOS and the normal direction of LOS, respectively, and $u_{ri} = \dot{v}_i\cos(q_i - \theta_{Ti}) + v_i\dot{\theta}_{Ti}\sin(q_i - \theta_{Ti})$ and $u_{qi} = -\dot{v}_i\sin(q_i - \theta_{Ti}) + v_i\dot{\theta}_{Ti}\cos(q_i - \theta_{Ti})$ are the acceleration of the missile in the direction of the LOS and the normal direction of the LOS, respectively.

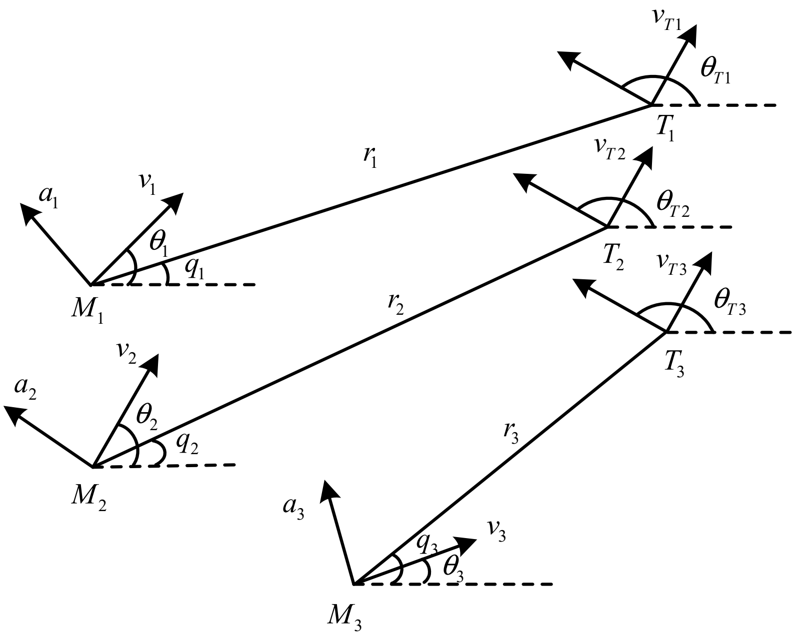

Figure 2. Two-dimensional geometry of the missile-target relative motion model.

Establish the nonlinear state equations of missile group member M_i, where $x_{1i} = r_i$, $x_{2i} = \dot{r}_i$, $x_{3i} = q_i - q_d$, $x_{4i} = \dot{q}_i$, and q_d is the desired terminal LOS of the missile M_i.

$$\begin{cases} \dot{x}_{1i} = x_{2i} \\ \dot{x}_{2i} = x_{1i}x_{4i}^2 - u_{ri} + w_{wi} \\ \dot{x}_{3i} = x_{4i} \\ \dot{x}_{4i} = -\dfrac{2x_{2i}}{x_{1i}}x_{4i} - \dfrac{u_{qi}}{x_{1i}} + \frac{w_{qi}}{x_{1i}} \end{cases} \tag{3}$$

Using Equation (3) to describe the multi-missile system can directly express the motion state of the missile and facilitate the design of the cooperative guidance law.

2.4. Analysis of Cooperative Guidance

In the guidance law design of time coordination and angle constraint, a common method is to design the controllers that independently control the flight time and the LOS according to the LOS direction and the normal direction of the LOS. Although this design is simple and there is no coupling in the controller design, the following three problems must be considered:

(1) The independently designed controllers only focus on the convergence speed and accuracy of their respective states, but there is a coupling between the missile flight states. The result of the LOS control will affect the time-to-go state. When the control

effects of the two controllers do not match, the missile will miss the target or cause significant bending or oscillation of the trajectory.

(2) To achieve good control, the output of the controller is often a large value in the initial stages of cooperation. However, in practice, the output capacity of the missile actuator is limited, and the theoretical guidance output cannot be achieved. This limitation will lead to a poor actual guidance effect or cause instability and non-convergence of the controller.

(3) In the case of the zero LOS constraint, the LOS and LOS rate will only converge to zero when the missile reaches to the same altitude as the target. In our experimental test, we found that the convergence time is the longest under the zero LOS constraint in angle-constrained guidance laws, and the ballistic trajectory is most likely to be significantly bent. Problems (1) and (2) are also the most prominent in this case.

In order to enable the multi-missile to simultaneously intercept the target with zero LOS and the same speed, this paper considers the acceleration constraint and the three aspects described above. This paper designs the cooperative guidance law in two parts: the first part designs the controller of the LOS direction to realize the impact time and speed coordination of multiple missiles. The second part designs the controller in the normal direction of the LOS to satisfy the constraint of zero LOS.

3. Multi-Missile Cooperative Guidance Law Design

3.1. Guidance Law Design in the LOS Direction

3.1.1. Multi-Agent Consistency Theory

In the time-coordinated interception of missiles, the communication network is used for inter-missile communication, and information such as the missile-target distance and time-to-go of other missiles is obtained to adjust its own speed. The communication topology between missiles can be described by an undirected graph, $G(v, \varepsilon, A)$, where $v = \{v_1, v_2, \ldots, v_n\}$ represents a group of communication nodes, the edge $\varepsilon = v \times v$ represents the connection between nodes, and the adjacency matrix $A = [\alpha_{ij}]$ represents the communication capability between missiles. If missile i and missile j can communicate with each other, then $\alpha_{ij} = 1$, otherwise $\alpha_{ij} = 0$, let $\alpha_{ii} = 0$. If any two nodes in G can find a path to connect them, it is said to be connected. That is, any missile can directly or indirectly cooperate with all other missiles.

Lemma 1 ([15])**.** *Finite-time consensus: for a multi-agent system composed of n agents, the state equation of each agent is as follows:*

$$\dot{x}_i = u_i \tag{4}$$

where x_i is the state of agent i and u_i is the consistency protocol, which is the function of state variables. If under any initial conditions and for any agent j there exists a finite time t^* such that when $t \geq t^*$,$x_j(t) = x^*$ holds, where x^* is a real number, then u_i is called a finite-time consensus protocol.

Lemma 2 ([37])**.** *Considering the system composed of n agents with state $\dot{x} = u_i$, when $G(v, \varepsilon, A)$ is undirected and connected, the following consistency protocol u_i can ensure the uniform convergence of multi-agent states in finite time:*

$$u_i = \operatorname{sgn}\left(\sum_{j=1}^{n} \alpha_{ij}(x_i - x_j)\right)\left|\sum_{j}^{n} \alpha_{ij}(x_i - x_j)\right|^{\alpha_i} \tag{5}$$

where α_{ij} is the element in adjacency matrix A , α_i is a constant, and $0 < \alpha_i < 1$.

3.1.2. Impact Time and Speed Consistency Control of Multi-Missiles

According to Lemma 2, the consistency protocol is used to design a controller u_i to control the convergence consistency of the multi-agent state x_i. However, the consistency protocol can only control the convergence of a single state. Scholars often use this consistency protocol to realize the time coordination of multiple missiles. However, the operational pattern of this paper requires two constraints: multiple mother-cabins must reach the "release point" at the same time, and the speed must converge to a consistent value. One way to achieve this goal is to design controllers for missile speed and time-to-go to control the two states and to achieve consistency, respectively. However, if the two controllers are superimposed in the LOS direction at the same time, coupling will inevitably occur. As a result, the "consistent convergence in finite time" of the consensus protocol no longer holds, and the finite-time convergence of the controllers cannot be proven.

In view of this, we will not directly apply the consistency protocol (5), but instead try to imitate the form of Equation (5) to design the LOS direction controller hoping to achieve the convergence of both time-to-go and speed. Due to the zero LOS constraint, the missile will fly to the same altitude as the target in a short time. In addition, there is speed coordination among multiple missiles. Theoretically, the time coordination can be achieved only by taking the relative distance r_i between the missile and the target as the coordination variable. Therefore, under the condition that multiple missiles are expected to impact the target at the same speed and time, the missile speed v_i and the missile-target distance r_i are taken as the coordination variables, and the controller is obtained by imitating the form of consistency protocol (5):

$$\overline{u}_{ri} = \mathrm{sgn}\left(\sum_{j=1}^{n} \alpha_{ij}\left[(r_i - r_j) + (v_i - v_j)\right]\right) \times \left|\sum_{j=1}^{n} \alpha_{ij}\left[(r_i - r_j) + (v_i - v_j)\right]\right|^{\alpha_i} \tag{6}$$

where α_{ij} represents the communication capability between missile i and j, α_i is a constant, and $0 < \alpha_i < 1$.

During the test, it was found that directly taking the speed as the coordination variable in the controller (6) resulted in a large overshoot and frequent switching, which in turn led to a longer convergence time.

In this regard, it was experimentally determined that adding the time-to-go coordination variable $t_{go,i}$ could effectively suppress the overshoot, and replacing the coordination variable v_i with $\dot{r}_i$ could make the output of the controller smoother. The resulting controller has a simple structure, the controller output is small in the middle and rear sections of the guidance, has a smooth gradient, and can ensure that the missile speed and time-to-go converge to the same value upon impact. The designed controller is as follows:

$$\begin{aligned} \overline{u}_{ri} = \mathrm{sgn} \quad & \left(\sum_{j=1}^{n} \alpha_{ij}\left[(r_i - r_j) + (\dot{r}_i - \dot{r}_j) + V_{\mathrm{m}}(t_{go,i} - t_{go,j})\right]\right) \times \\ & \left|\sum_{j=1}^{n} \alpha_{ij}\left[(r_i - r_j) + (\dot{r}_i - \dot{r}_j) + V_{\mathrm{m}}(t_{go,i} - t_{go,j})\right]\right|^{\alpha_i} \end{aligned} \tag{7}$$

where V_m is the average velocity of the missile, which is regarded as a constant in the controller and can be set after the performance parameters of the missile are determined.

During the actual missile target approach, the derivative of the distance between the missile and the target changes slightly, and $t_{go,i}$ can be calculated by the following equation [16]:

$$t_{go,i} = -\frac{r_i}{\dot{r}_i} \tag{8}$$

This time-to-go calculation method is simple and effective and is suitable for small maneuvering targets such as UAV clusters.

The overload constraint is added to the controller (7) to obtain the LOS direction controller as follows:

$$u_{ri} = \begin{cases} \overline{u}_{ri}, & |\overline{u}_{ri}| \leq u_{ri\max} \\ \mathrm{sgn}(\overline{u}_{ri}) \cdot u_{ri\max}, & |\overline{u}_{ri}| > u_{ri\max} \end{cases} \tag{9}$$

where $u_{ri\max}$ is the ultimate overload that missile i can provide in the LOS direction.

3.2. Guidance Law Design in the Normal Direction of LOS

The last two equations in the missile-target movement model (3) are taken as the missile-target sight angle system and written in the form of the LOS overload constrained as:

$$\begin{cases} \dot{x}_{3i} = x_{4i} \\ \dot{x}_{4i} = -\frac{2x_{2i}}{x_{1i}} x_{4i} - \frac{sat(u_{qi})}{x_{1i}} + \frac{w_{qi}}{x_{1i}} \end{cases} \tag{10}$$

where the saturation function $sat(u_{qi})$ is defined as:

$$sat(u_{qi}) = \begin{cases} u_{qi}, & |u_{qi}| \le u_{qi\max} \\ \mathrm{sgn}(u_{qi}) \cdot u_{qi\max}, & |u_{qi}| > u_{qi\max} \end{cases} \tag{11}$$

where $u_{qi\max}$ is the ultimate overload that missile i can provide in the direction of the LOS.

The sliding surface with the LOS constraint is usually designed as $s = k\dot{q} + q$, where k is the coefficient of LOS change rate, and the proportion of LOS and LOS rate in the sliding surface is constant.

Under the constraint of zero LOS, the trajectory will bend sharply due to the rapid convergence of the LOS. To obtain a smoother trajectory, the following adaptive sliding surface is designed:

$$s_i = K_i \dot{q}_i + q_i \tag{12}$$

where K_i is the adaptive coefficient, which is obtained from the following equation:

$$K_i = 10\hat{}\left(\frac{r_i}{r_{i0}}\right)^2 - 0.8 \tag{13}$$

In Equation (13), r_{i0} and r_i are the initial missile-target distance and the real-time missile-target distance, respectively. This design sets the LOS rate $\dot{q}_i$ as the main guide term when the missile-target distance is far to avoid an overly curved trajectory. When the missile-target distance is close, the LOS error q_i is the main guide term to make a rapid response to the target maneuver. Considering the simplicity of the controller expression, K_i is regarded as a constant in the derivation of the controller.

Remark 3. *When i takes different values, the expression of the sliding mode variable s_i is the same. For readability, s_i in the following text does not have a subscript.*

For the sliding mode control with the LOS constraint, it is hoped that the approach speed of the sliding mode surface can be controlled, and the chattering of the control output is small to ensure the flight reliability of the missile. Based on this consideration, this paper selects a fast power reaching law as follows [38]:

$$\dot{s} = -k_1 s - k_2 |s|^{\beta_i} \mathrm{sgn}(s) \tag{14}$$

where $k_1 > 0$, $k_2 > 0$, and $0 < \beta_i < 1$. This reaching law is a combination of the exponential reaching law and power reaching law. It can be seen from Equation (14) that $-k_1 s$ plays a major role in the initial stage of guidance because the sliding mode variable s is large; as the missile approaches the target and the guidance error decreases, the approach speed primarily depends on $-k_2|s|^{\beta_i}\mathrm{sgn}(s)$. Choosing smaller k_1 and β_i values and a larger k_2 value, we can achieve a relatively smooth trajectory and can make a quick responses to the target maneuver when approaching the target.

Combining Equations (12) and (14), and LOS system (10), the LOS normal direction controller is obtained as:

$$u_{qi} = x_{1i}\left(-\frac{2x_{2i}}{x_{1i}}x_{4i} + \frac{x_{4i} + k_1 s + k_2|s|^{\beta_i}\mathrm{sgn}(s)}{K_i} + \frac{w_{qi}}{x_{1i}}\right) \tag{15}$$

Note that Equation (15) contains the uncertainty variables w_{qi}/x_{1i}, which can be regarded as the disturbance in the system, where w_{qi} is the normal acceleration of the target in the LOS, which is difficult to observe directly. An effective method is to use the observer to estimate the disturbance in the system.

Lemma 3 ([39])**.** *For first-order SISO nonlinear systems,*

$$\dot{\sigma} = u + d \tag{16}$$

where σ is the state variable, u is the control input, and d is the system interference. An inhomogeneous high-order sliding mode disturbance observer of the form

$$\begin{cases} \dot{z}_0 = v_0 + u, v_0 = h_0(z_0 - \sigma) + z_1 \\ \dot{z}_1 = v_1, \qquad v_1 = h_1(z_1 - v_0) + z_2 \\ \vdots \\ \dot{z}_{m-1} = v_{m-1}, v_{m-1} = h_{m-1}(z_{m-1} - v_{m-2}) + z_m \\ \dot{z}_m = h(z_m - v_{m-1}) \end{cases} \tag{17}$$

where the expression of function h is as follows:

$$h_i(\cdot) = -\lambda_i L^{1/(m-i+1)}\left|\cdot\right|^{(m-i)/(m-i+1)}\mathrm{sgn}(\cdot) - \mu_i(\cdot) \tag{18}$$

where $\lambda_i > 0$, $\mu_i > 0$, $i = 0, 1, \ldots, \mathrm{m}$, and L is the Lipschitz constant. Based on the observer, the estimation error can be eliminated in a finite time, i.e., $z_0 = \sigma$, $z_1 = d$, …, $z_m = \sigma_m - d^{(m-1)}$.

Combined with system (10), Lemma 3 is applied to design an inhomogeneous disturbance observer (see Equation (19)) to estimate w_{qi}/x_{1i}:

$$\begin{cases} \dot{z}_{0i} = v_{0i} - \frac{2x_{2i}}{x_{1i}}x_{4i} - \frac{u_{qi}}{x_{1i}} \\ v_{0i} = -\lambda_{2i}L_i^{\frac{1}{3}}|z_{0i} - x_{4i}|^{\frac{2}{3}}\mathrm{sgn}(z_{0i} - x_{4i}) - \mu_{2i}(z_{0i} - x_{4i}) + z_{1i} \\ \dot{z}_{1i} = v_{1i} \\ v_{1i} = -\lambda_{1i}L_i^{\frac{1}{2}}|z_{1i} - v_{0i}|^{\frac{1}{2}}\mathrm{sgn}(z_{1i} - v_{0i}) - \mu_{1i}(z_{1i} - v_{0i}) + z_{2i} \\ \dot{z}_{2i} = -\lambda_{0i}L_i\mathrm{sgn}(z_{2i} - v_{1i}) - \mu_{0i}(z_{2i} - v_{1i}) \\ \hat{d}_{qi} = z_{1i} \end{cases} \tag{19}$$

where $d_{qi} = w_{qi}/x_{1i}$ represents the system disturbance term, L_i is the constant satisfying $L_i > \left|\dot{d}_{qi}\right|$, and $\hat{d}_{qi}$ is the estimated value of the system disturbance.

Proof of the Controller (15). To prove the stability and finite-time convergence of controller (15), we introduce the following lemma. □

Lemma 4 ([19])**.** *Suppose $V(t)$ is a positive definite function, and there are constants $\mu, \eta > 0$* and $0 < \lambda < 1$ *such that $V(t)$ satisfies the following differential inequalities:*

$$\dot{V}(t) + \mu V(t) + \eta V^{\lambda}(t) \le 0 \tag{20}$$

Then the system will converge to zero in a finite time, and the convergence time satisfies the following constraint:

$$t_f \le t_0 + \frac{1}{\mu(1-\lambda)} \ln \frac{\mu V^{1-\lambda}(t_0) + \eta}{\eta} \tag{21}$$

The Lyapunov function V is selected as:

$$V = \frac{1}{2}s^2 \tag{22}$$

By differentiating Equation (22), we obtain:

$$\begin{aligned} \dot{V} &= s\dot{s} = -k_1 s^2 - k_2|s|^{\beta_i} s\mathrm{sgn}(s) \\ &= -k_1 s^2 - k_2|s|^{\beta_i+1} \\ &= -\mu V - \eta V^{\eta} \le 0 \end{aligned} \tag{23}$$

where $\mu = 2k_1 > 0$, $\eta = 2^{\frac{\beta_i+1}{2}} k_2$, and $0 < \lambda = \frac{\beta_i+1}{2} < 1$. According to Lemma 4, the sliding mode surface s is reachable in a limited time, and the LOS and LOS rate of each missile converges to zero in a limited time.

Theorem 1. *Considering the multi-missile system (3), when the communication topology graph G is undirected and connected, the controller (9) and the controller (15) can make the multi-missile system impact the target at the same time. The LOS of each missile converges to zero in a finite time, and the speed converges at the impact time.*

Remark 4. *The controllers designed in this paper contain the symbolic function* $\mathrm{sgn}(\cdot)$*, which may cause chattering in the output of the controller. Therefore, the following function* $h(\cdot)$*is designed to replace the original symbolic function:*

$$h(x) = \frac{2}{1+e^{-10x}} - 1 \tag{24}$$

3.3. Multi-Missile Cooperative Guidance Structure

Shiyu Zhao et al. designed a two-layer cooperative guidance structure [7] composed of two different control strategies. The upper layer is the coordination layer, which receives the coordination variable information based on the centralized or distributed communication network topology and obtains the expected coordination variable based on the coordination strategy. The lower layer is the control layer, which combines with the expected coordination variables generated by the coordination layer to form the local guidance law of each missile. The coordination variables refer to the minimum information required to achieve the collaborative tasks. The guidance structure can achieve multi-missile coordination by converging the coordination variables of each missile to the expected coordination variables. It has the advantages of a clear structure and good universality and can be better applied to the multi mother-cabin guidance without a leader-follower relationship, as discussed in this paper.

The cooperative guidance structure in this paper is designed based on the two-layer cooperative guidance structure, as shown in Figure 3. The coordination strategy (Equation (7)) in this paper cannot obtain the expected coordination variables, but directly obtains the control output u_{ri} that can control the coordination variables $t_{go,i}$ and v_i to achieve consistency. u_{ri} is transferred to the control layer, where it is combined with the guidance law u_{qi} with zero LOS constraint of each missile to form the local guidance law u_i of each missile.

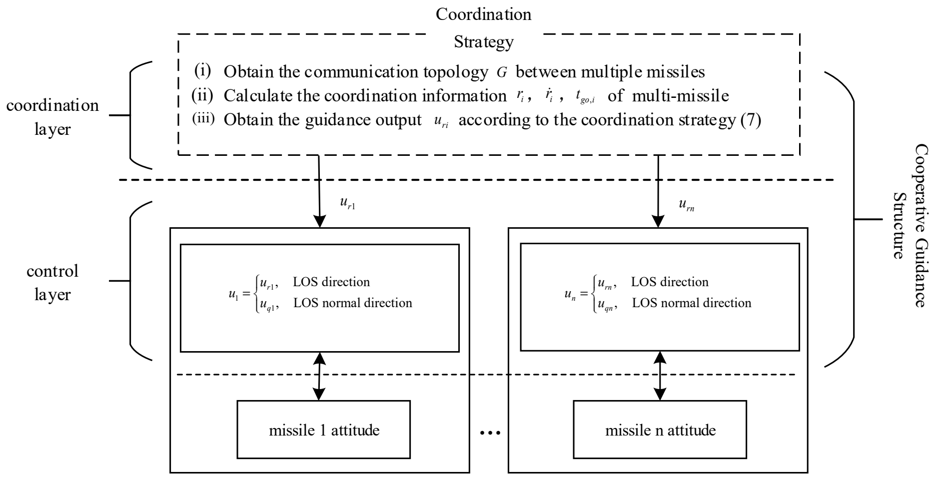

Figure 3. Multi-missile cooperative guidance structure.

4. Simulations

This section verifies the designed cooperative guidance law. Taking the cooperative interception of UAV clusters by three mother-son missiles as an example, it is required that the three mother-cabins reach the "release point" at the same time with zero LOS and the same speed. The communication topology G between the three missiles is shown in Figure 4. The maximum overload in the LOS direction of the missile is 5 g, the maximum overload in the normal direction of the LOS is 10 g, g = 9.8 m/s^2, and the simulation step length is 0.01 s.

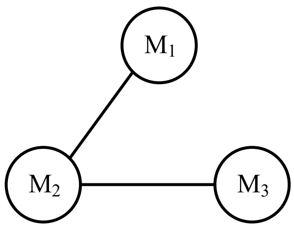

Figure 4. Communication topology of three missiles.

Guidance law parameters are set as follows: parameter setting of controller (9): $\alpha_i = 0.8$, $V_m = 500$ Parameter setting of controller (15): $k_1 = 1$, $k_2 = 5$, $\beta_i = 0.2$. Disturbance observer (19) parameters: $\lambda_{0i} = 1.5$, $\lambda_{1i} = 2$, $\lambda_{2i} = 3$, $\mu_{0i} = 3$, $\mu_{1i} = 4$, $\mu_{2i} = 5$, $L_i = 1$, where $i = 1, 2, 3$.

Two scenarios are used to verify the performance of the guidance law, target non-maneuver and circular maneuver, and different initial states of the missiles and targets are set. Note: the "targets" here represents the "release points", and the "missiles" here represents the "mother-cabins".

Scenario 1: The targets do not maneuver, and the initial state of the missiles and targets is shown in Table 1.

The simulation results are shown in Figure 5.

Table 1. Initial state setting of missiles and targets.

Initial Position/m	Initial Speed/m·s^{-1}	Initial Heading Angle/°
Missile 1	(−1000, 2100)	520
Missile 2	(0, 1900)	500
Missile 3	(0, 1100)	470
Target 1	(25,000, 1800)	200
Target 2	(27,000, 1600)	200
Target 3	(25,000, 1400)	200

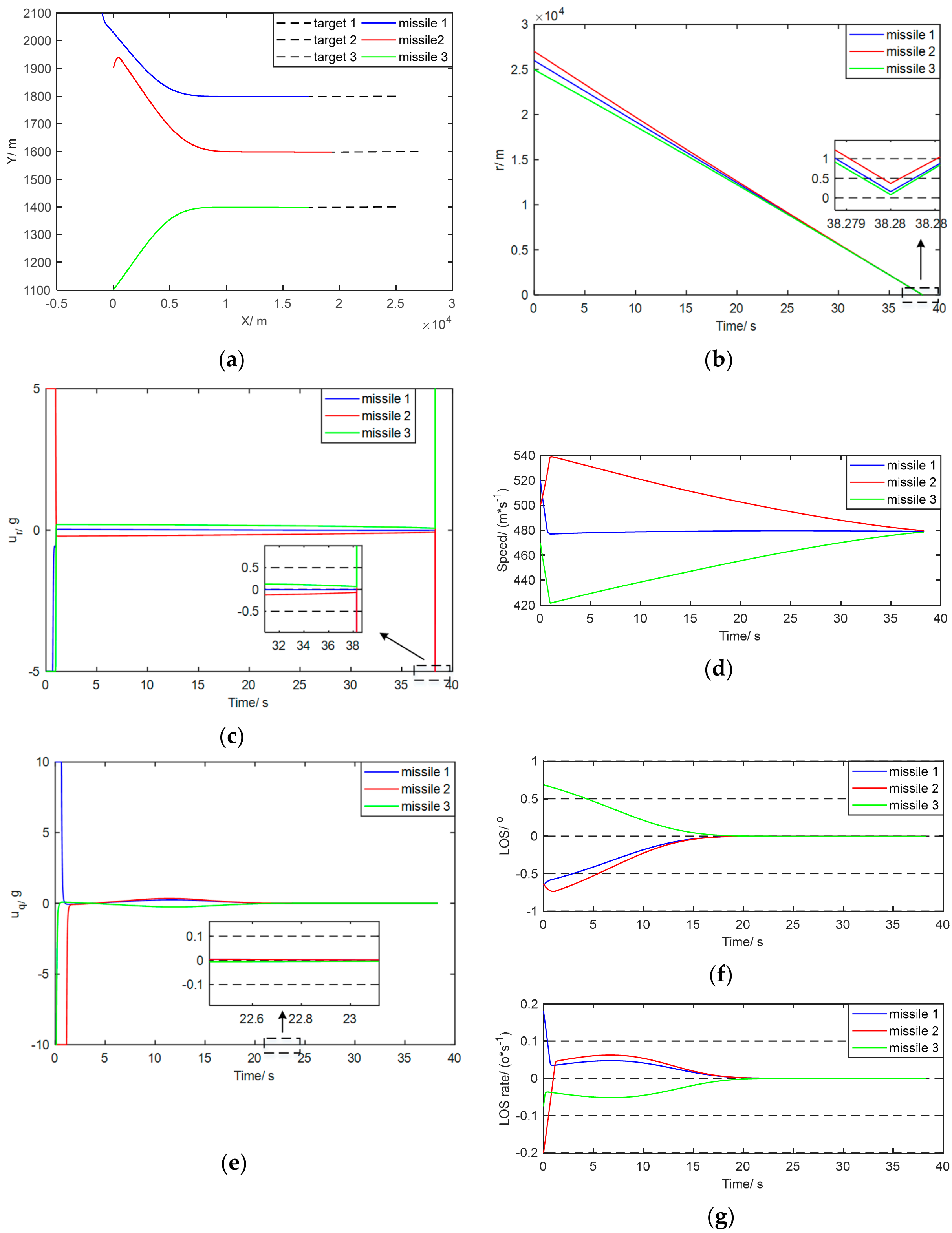

Figure 5. Simulation results of target non-maneuver. (**a**) Missile-target trajectory; (**b**) missile-target relative distances; (**c**) overload on the LOS direction; (**d**) speed convergence curve; (**e**) overload on the normal direction of LOS; (**f**) LOS convergence curve; (**g**) LOS rate convergence curve.

As can be seen from Figure 5a,b, except for missile 2 needing to complete a quick turn at the initial phase for heading angle adjustment, all three missiles can obtain a smooth trajectory under the action of the controller and can impact the targets simultaneously in

38.28 s, with misses of less than 0.5 m. As can be seen from Figure 5c,d, due to the large difference in the initial time-to-go, the three missiles need to quickly adjust their speed in the initial phase. However, after approximately 2 s, the convergence process becomes very smooth, and the time-to-go and speed converge to the same only at the time of impact. This allows the controller to meet the guidance requirements with only a small, continuous, and smooth output. As can be seen from Figure 5b,e,f, the overload in the normal LOS direction of the missiles is saturated in the initial phase so that the missiles can quickly adjust to the desired attitude. Then, the controller only needs to adjust the output in a small range according to the motion state of the missile-target. The subsequent output after approximately 2 s is small and there is no chattering, which ensures a relatively flat trajectory. The LOS and the LOS rate can both converge to zero in approximately 20 s.

In conclusion, Figure 5 shows that the missiles can quickly meet the zero LOS constraint while ensuring a smoother trajectory, which creates good conditions for the seeker to detect the cluster target. The controller adjusts the speed slowly and steadily to ensure that the output of the controller is small and continuous. In the initial phase, the output of the two controllers is saturated so that the missiles can adjust to the desired attitude as quickly as possible, allowing them to better cope with the possible subsequent maneuvering of the targets. The subsequent output is small and there is no chattering, which can save energy and ensure flight stability.

Scenario 2: The targets do a circular maneuver with an acceleration of 2 $m^2 \cdot s^{-1}$. The initial state of the missiles and targets is shown in Table 2.

Table 2. Initial state setting of missiles and targets.

Initial Position/m	Initial Speed/m·s^{-1}	Initial Heading Angle/°
Missile 1	(−500, 2200)	500
Missile 2	(800, 1800)	530
Missile 3	(0, 1000)	480
Target 1	(28,000, 1600)	200
Target 2	(25,000, 1500)	200
Target 3	(23,000, 1300)	200

The simulation results are shown in Figure 6.

As can be seen from Figure 6a,b, except for missile 3 needing to complete a quick turn at the initial stage due to the heading angle adjustment, the three missiles can obtain a smooth trajectory under the action of the controller and can impact the target simultaneously in 38.70 s, with misses less than 1 m. Figure 6c,g shows that the output characteristics of the controller and the convergence characteristics of the missile state are similar to those when the targets are not maneuvering. It can be seen that after adjusting the initial state of the missiles, targets, and the maneuvering situation of the targets, the designed guidance law still performs well.

Table 3 shows that under the two targets maneuvering conditions, the misses of each missile are less than 1 m, that is, allowing each mother-cabin to fly to the "release point" with a small deviation. In addition to the convergence of the LOS to zero, which satisfies the detection conditions of the seeker for the UAV cluster, it is also necessary to pay attention to the heading angle of the mother-cabins at the "release point". When the target is not maneuvering, the heading angle of each missile can converge to zero. When the target is maneuvering in a circular pattern with an acceleration of 2 $m^2 \cdot s^{-1}$, the heading angles of the three missiles are all maintained at a value of approximately -9° to respond to the targets' maneuvering. It can be assumed that the initial velocity of the son-interceptors is aligned with the targets after release and is capable of completing the follow-on interception.

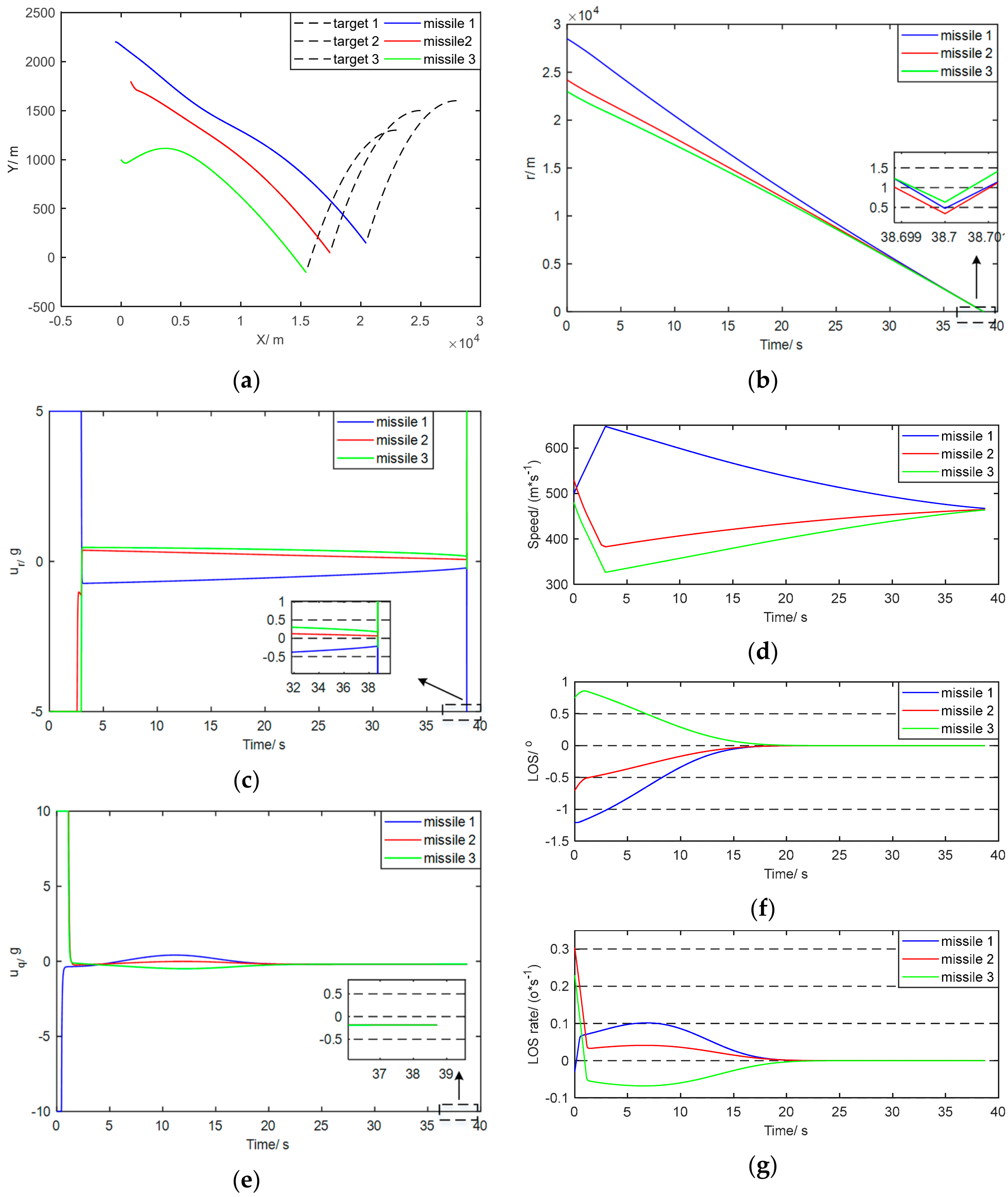

Figure 6. Simulation results of the target circular maneuver. (**a**) Missile-target trajectory; (**b**) missile-target relative distances; (**c**) overload on the LOS direction; (**d**) speed convergence curve; (**e**) overload on the normal direction of LOS; (**f**) LOS convergence curve; (**g**) LOS rate convergence curve.

Table 3. Guidance results.

Targets Maneuver	Missiles	Misses/m	Intercept Time/s	Missile Heading Angle/°
Non-maneuver	Missile 1	0.16	38.28	0
	Missile 2	0.37		0
	Missile 3	0.08		0
circular maneuver	Missile 1	0.47	38.70	−9.13
	Missile 2	0.34		−9.18
	Missile 3	0.63		−9.20

Combining Figures 5 and 6 with Table 3, it can be seen that the designed multi-missile cooperative guidance law is well-suited to the mother-cabin guidance in this operational pattern, with the advantages of a smooth trajectory and a small, non-chattering controller output.

5. Conclusions

Based on the operational pattern of multi mother-son missile intercept UAV clusters, this paper proposes a special cooperative guidance law for the interception of UAV clusters by mother-son missiles. The proposed method includes some innovative designs, such as using the time-to-go and the derivative of the missile-target distance as the coordination variable to suppress the overshoot of speed. These designs ensure that the missile speed converges uniformly at the time of impacting the target, resulting in small, smooth, and stable controller output amplitudes, which saves fuel and ensures flight reliability to some extent. The variable coefficient of the adaptive sliding mode is designed so that a relatively smooth trajectory can be obtained under the constraint of zero LOS. Finally, the effectiveness of the proposed method was verified by simulations.

Author Contributions: Conceptualization, R.L. and G.H.; methodology, R.L. and X.B.; software, R.L.; validation, R.L., X.B. and J.S.; writing—original draft preparation, R.L. and J.S.; writing—review and editing, R.L.; supervision, G.H. All authors have read and agreed to the published version of the manuscript.

Funding: This work was supported by the National Natural Science Foundation of China (Grant No. 61703424).

Institutional Review Board Statement: No applicable.

Informed Consent Statement: No applicable.

Data Availability Statement: All the data used to support the findings of this study are included within the article.

Conflicts of Interest: The authors declare no conflict of interest.

References

1. Jeon, I.S.; Lee, J.I.; Tahk, M.J. Impact-time-control guidance law for anti-ship missiles. *IEEE Trans. Control Syst. Technol.* **2006**, *14*, 260–266. [CrossRef]
2. Lee, J.I.; Jeon, I.S. Guidance law to control impact time and angle. *IEEE Trans. Aerosp. Electron. Syst.* **2007**, *43*, 301–310.
3. Zhang, Y.A.; Ma, G.X.; Liu, A.L. Guidance law with impact time and impact angle constraints. *Chin. J. Aeronaut.* **2013**, *26*, 960–966. [CrossRef]
4. Kim, M.; Jung, B.; Han, B.; Lee, S.; Kim, Y. Lyapunov-Based Impact Time Control Guidance Laws Against Stationary Targets. *IEEE Trans. Aerosp. Electron. Syst.* **2015**, *51*, 1111–1122. [CrossRef]
5. Zhao, J.B.; Yang, S.X. Review of multi-missile cooperative guidance. *Acta Aeronaut. Astronaut. Sin.* **2017**, *38*, 22–34. (In Chinese)
6. Zhang, Y.A.; Ma, G.X.; Wang, X.P. Time-cooperative guidance for multi-missiles: A leader-follower strategy. *Acta Aeronaut. Astronaut. Sin.* **2009**, *30*, 1109–1118. (In Chinese)
7. Zhao, S.Y.; Zhou, R. Multi-missile cooperative guidance using coordination variables. *Acta Aeronaut. Astronaut. Sin.* **2008**, *29*, 1605–1611. (In Chinese)
8. Yu, J.L.; Dong, X.W.; Li, Q.D.; Lv, J.H.; Ren, Z. Distributed adaptive cooperative time-varying formation tracking guidance for multiple aerial vehicles system. *Aerosp. Sci. Technol.* **2021**, *117*, 17. [CrossRef]
9. Sun, X.J.; Zhou, R.; Wu, J.; Chen, S.D. Distributed cooperative guidance and control for multiple missiles. *J. Beijing Univ. Aeronaut. Astronaut.* **2014**, *40*, 120–124. (In Chinese)
10. Zhao, Q.L.; Chen, J.; Dong, X.W.; Li, Q.D.; Ren, Z. Cooperative guidance law for heterogeneous missiles intercepting hypersonic weapon. *Acta Aeronaut. Astronaut. Sin.* **2016**, *37*, 936–948. (In Chinese)
11. Cong, M.Y.; Cheng, X.H.; Zhao, Z.Q.; Li, Z.J. Studies on Multi-Constraints Cooperative Guidance Method Based on Distributed MPC for Multi-Missiles. *Appl. Sci.* **2021**, *11*, 10857. [CrossRef]
12. Kumar, S.R.; Ghose, D. Cooperative Rendezvous Guidance using Sliding Mode Control for Interception of Stationary Targets. *IFAC Proc. Vol.* **2014**, *47*, 477–483. [CrossRef]
13. Zhao, J.; Zhou, R. Unified approach to cooperative guidance laws against stationary and maneuvering targets. *Nonlinear Dyn.* **2015**, *81*, 1635–1647. [CrossRef]

14. Chen, Z.Y.; Yu, J.L.; Dong, X.W.; Ren, Z. Three-dimensional cooperative guidance strategy and guidance law for intercepting highly maneuvering target. *Chin. J. Aeronaut.* **2021**, *34*, 485–495. [CrossRef]
15. Wang, L.; Xiao, F. Finite-Time Consensus Problems for Networks of Dynamic Agents. *IEEE Trans. Autom. Control* **2010**, *55*, 950–955. [CrossRef]
16. Zhang, P.; Liu, H.H.T.; Li, X.B.; Yao, Y. Fault tolerance of cooperative interception using multiple flight vehicles. *J. Frankl. Inst.-Eng. Appl. Math.* **2013**, *350*, 2373–2395. [CrossRef]
17. Ma, S.; Wang, X.G.; Wang, Z.Y.; Chen, Q. Consensus-Based Finite-Time Cooperative Guidance with Field-of-View Constraint. *Int. J. Aeronaut. Space Sci.* **2022**, *23*, 966–979. [CrossRef]
18. An, K.; Guo, Z.Y.; Huang, W.; Xu, X.P. A Cooperative Guidance Approach Based on the Finite-Time Control Theory for Hypersonic Vehicles. *Int. J. Aeronaut. Space Sci.* **2022**, *23*, 169–179. [CrossRef]
19. Song, J.H.; Song, S.M.; Zhou, H.B. Adaptive Nonsingular Fast Terminal Sliding Mode Guidance Law with Impact Angle Constraints. *Int. J. Control Autom. Syst.* **2016**, *14*, 99–114. [CrossRef]
20. He, S.M.; Lin, D.F. Adaptive nonsingular sliding mode based guidance law with terminal angular constraint. *Int. J. Aeronaut. Space Sci.* **2014**, *15*, 146–152. [CrossRef]
21. Yang, X.Y.; Song, S.M. Three-dimensional consensus algorithm for nonsingular distributed cooperative guidance strategy. *Aerosp. Sci. Technol.* **2021**, *118*, 18. [CrossRef]
22. Shtessel, Y.B.; Moreno, J.A.; Fridman, L.M. Twisting sliding mode control with adaptation: Lyapunov design, methodology and application. *Automatica* **2017**, *75*, 229–235. [CrossRef]
23. Zhang, S.; Guo, Y.; Liu, Z.G.; Wang, S.C.; Hu, X.X. Finite-Time Cooperative Guidance Strategy for Impact Angle and Time Control. *IEEE Trans. Aerosp. Electron. Syst.* **2021**, *57*, 806–819. [CrossRef]
24. Ma, M.C.; Song, S.M. Three-dimensional prescribed performance cooperative guidance law with spatial constraint for intercepting manoeuvring targets. *Int. J. Control* **2022**, 1–12. [CrossRef]
25. Bu, X.W.; Jiang, B.X.; Lei, H.M. Performance Guaranteed Finite-Time Non-Affine Control of Waverider Vehicles Without Function-Approximation. *IEEE Trans. Intell. Transp. Syst.* **2023**, *24*, 3252–3262. [CrossRef]
26. Bu, X.W.; Jiang, B.X.; Lei, H.M. Non-fragile Quantitative Prescribed Performance Control of Waverider Vehicles With Actuator Saturation. *IEEE Trans. Aerosp. Electron. Syst.* **2022**, *58*, 3538–3548. [CrossRef]
27. Bu, X.W.; Hua, C.C.; Lv, M.L.; Wu, Z.H. Flight Control of Waverider Vehicles with Fragility-avoidance Prescribed Performance. *IEEE Trans. Aerosp. Electron. Syst.* **2023**. [CrossRef]
28. Bu, X.W.; Lv, M.L.; Lei, H.M.; Cao, J.D. Fuzzy Neural Pseudo Control With Prescribed Performance for Waverider Vehicles: A Fragility-avoidance Approach. *IEEE Trans. Cybern.* **2023**. [CrossRef]
29. Bu, X.W.; Jiang, B.X.; Lei, H.M. Low-complexity Fuzzy Neural Control Of Constrained Waverider Vehicles Via Fragility-free Prescribed Performance Approach. *IEEE Trans. Fuzzy Syst.* **2022**. [CrossRef]
30. Li, G.F.; Lu, J.H.; Zhu, G.L.; Liu, K.X. Distributed observer-based cooperative guidance with appointed impact time and collision avoidance. *J. Frankl. Inst.-Eng. Appl. Math.* **2021**, *358*, 6976–6993. [CrossRef]
31. Mukherjee, D.; Kumar, S.R. Finite-Time Heterogeneous Cyclic Pursuit With Application to Cooperative Target Interception. *IEEE Trans. Cybern.* **2022**, *52*, 11951–11962. [CrossRef] [PubMed]
32. Tao, G. Model reference adaptive control with L $1+\alpha$ tracking. *Int. J. Control* **1996**, *64*, 859–870. [CrossRef]
33. Hosseinzadeh, M.; Yazdanpanah, M.J. Performance enhanced model reference adaptive control through switching non-quadratic Lyapunov functions. *Syst. Control Lett.* **2015**, *76*, 47–55. [CrossRef]
34. Li, J.J.; Luo, C.X.; Huang, W. "Bee Catching": System Conception of Air Short Range Anti-UAV Bee Colony. *Mod. Def. Technol.* **2020**, *48*, 16–22. (In Chinese)
35. Gao, X.Z.; Wang, K.L.; Peng, X.; Guo, Z.; Hou, Z.X. Drone-smasher: The key technology analysis on the manner of hard kill to counter UAV swarm. *Natl. Def. Technol.* **2020**, *41*, 33–38. (In Chinese)
36. Yan, J.D.; Xie, H.B.; Zhaung, D.Y. Research on threat and countermeasures of UAV cluster for key position air-defense. *Aerodyn. Missile J.* **2021**, 56–61. (In Chinese) [CrossRef]
37. Song, J.H.; Song, S.M.; Xu, S.L. A Cooperative Guidance Law for Multiple Missiles to Intercept Maneuvering Target. *J. Astonautics* **2016**, *37*, 1306–1314. (In Chinese)
38. Yu, S.H.; Yu, X.H.; Shirinzadeh, B.; Man, Z.H. Continuous finite-time control for robotic manipulators with terminal sliding mode. *Automatica* **2005**, *41*, 1957–1964. [CrossRef]
39. Taleb, M.; Plestan, F. Adaptive robust controller based on integral sliding mode concept. *Int. J. Control* **2016**, *89*, 1788–1797. [CrossRef]